Journal of Solid State Chemistry 183 (2010) 228–233

Contents lists available at ScienceDirect

Journal of Solid State Chemistry

journal homepage: www.elsevier.com/locate/jssc

Polyoxometalate-based eight-connected self-catenated network and fivefold interpenetrating framework

Zhiming Zhang, Jia Liu, Yangguang Li, Shuang Yao, Enbo Wang *, Xinlong Wang

Key Laboratory of Polyoxometalate Science of Ministry of Education, Department of Chemistry, Northeast Normal University, Ren Min Street No. 5268, Changchun, Jilin 130024, PR China

ARTICLE INFO

Article history:
Received 30 May 2009
Received in revised form
20 October 2009
Accepted 26 October 2009
Available online 31 October 2009

Keywords:
Polyoxometalate
Entangled structure
Self-penetrating

ABSTRACT

Two entangled compounds $[(bpy)_6Cu^{I}_6Cl_3(Mo^{V}W_5O_{19})]$ (**1**) and $[(bpy)_7Cu^{I}_7Cl_2(BW_{12}O_{40})]\cdot H_2O$ (**2**) (bpy=4,4′-bipyridine), have been successfully synthesized under hydrothermal conditions and characterized by element analysis, IR spectroscopy, thermal gravimetric analysis, X-ray photoelectron spectroscopy, and single crystal X-ray diffraction analyses. Compound **1** represents the first eight-connected self-penetrating network constructed from cuprous chloride clusters $[Cu_6Cl_3]$ and Lindquist-type polyoxoanions. Compound **2** exhibits an interesting fivefold interpenetrating network consisting of Keggin polyoxoanions and Cu^{+}-metal–organic framework. Crystal data of the two compounds are following: **1**, triclinic, $P1$, a=11.502(2) Å, b=13.069(3) Å, c=13.296(3) Å, α=90.55(3)°, β=113.74(3)°, γ=110.48(3)°, Z=1; **2**, triclinic, $P1$, a=12.341(3) Å, b=13.119(3) Å, c=15.367(3) Å, α=99.12(3)°, β=90.53(3)°, γ=104.49(3)°, Z=1.

1. Introduction

Entanglements are common in biology as seen in catenanes, rotaxanes and molecular knots, which have attracted considerable attention not only for their potential applications as functional solid materials, but also for their intriguing architectures and topologies [1–5]. In this field, the self-catenation nets, with smallest topological rings catenated by other rings belonging to the same network, represent an important subfamily, which have provided a long-standing fascination for chemists [6,7]. However, the self-catenation nets are rarely reported and still a challenging issue in the coordination chemistry.

Polyoxometalates (POMs), as their controllable shape, size, high-negative charges, oxo-riched surfaces, and interesting physical and chemical properties [8–10], have been proved to be one of the excellent candidates to construct extended organic–inorganic hybrid materials. Up to now, a large number of extended organic–inorganic hybrid materials composed of POM building blocks, linked by organic ligands or metal–organic coordination complexes have been reported, which possess of variety of applications in fields such as catalysis, electrical conductivity, gas storage and ion exchange [11,12]. As well known, the POM-based entangled system has far been unexplored and only a few examples have been documented up to now [13]. We have focused on entanglement system for a long time and obtained a series of entangled compounds: the interlocked and interdigitated architectures obtained by reaction of long flexible ligands and cadmium salts [14]; a series of entangled networks with inherent features of polycatenation, polythreading and polyknotting obtained by self-assembly of the rigid bpy, the long V-shaped 4,4′-oxybis(benzoate) ligands and Ni^{2+} [15]. Accordingly, we attempt to introduce the POMs into the entangled network system. Fortunately, several POM-based entangled structures were successfully obtained: a two fold interpenetrated diamondoid skeleton with the Keggin anions $[PMo_{12}O_{40}]^{3-}$ as guests [16], a three-connected fivefold interpenetrating network based on $[PW^{VI}_{10}W^{V}_{2}O_{40}]^{5-}$ building blocks [17], and a fourfold interpenetrating three-dimensional (3D) network composed of the $Cu[P_4Mo_6O_{25}(OH)_6]_2$ clusters covalently linked by Cu-bpy groups [18]. All these examples could confirm that POMs are suitable to construct entangled compounds; however, most POM-based entangled compounds are low connected coordination frameworks.

In this paper, we report an eight-connected self-catenated organic–inorganic hybrid and a fivefold interpenetrating 3D network based on the Lindquist-type anion $[Mo^{V}W_5O_{19}]^{3-}$ and the Keggin-type anion $[BW_{12}O_{40}]^{5-}$, respectively.

2. Experimental section

2.1. Materials

All chemicals were of analytical grade and obtained from commercial sources without further purification. $(NBu_4)_3$

* Corresponding author. Fax: +86 431 85098787.
E-mail address: wangeb889@nenu.edu.cn (E. Wang).

0022-4596/$ - see front matter Crown Copyright © 2009 Published by Elsevier Inc. All rights reserved.
doi:10.1016/j.jssc.2009.10.016

$[MoW_5O_{19}]$ and $K_5[BW_{12}O_{40}]\cdot 15H_2O$ was synthesized according to the literatures [19,20] and characterized by IR spectrum. Elemental analyses Mo, W and Cu were performed by a Leaman inductively coupled plasma (ICP) spectrometer; C, H and N were performed on a Perkin-Elmer 2400 CHN elemental analyzer. TG analyses were performed on a Perkin–Elmer TGA7 instrument in flowing N_2 with a heating rate of 10 °C min^{-1}. XPS analyses were performed on a VG ESCALABMKII spectrometer with an Mg$K\alpha$ (1253.6 eV) achromatic X-ray source. IR spectra were recorded in the range of 400–4000 cm^{-1} on an Alpha Centaurt FT/IR Spectrophotometer with pressed KBr pellets. Electrochemical experiments were carried out on a BAS Epsilon Analyzer. A conventional three-electrode system was used. The working electrode was compound **2** bulk-modified carbon paste electrode. A SCE was used as reference electrode and Pt gauze as a counter electrode.

2.2. Synthesis

Synthesis of **1**: A mixture of bpy (78 mg, 0.5 mmol), $CuCl_2\cdot 2H_2O$ (86 mg, 0.5 mmol), and H_2O (10 ml) was stirred for 10 min with heating at 60 °C. To this solution, $(NBu_4)_3[MoW_5O_{19}]$ (210 mg, 0.1 mmol) and NH_4Cl (53 mg, 1 mmol) were added. The pH value of the mixture was adjusted to 4.5 by addition of diluted HCl (1 mol/L). Then, the mixture was transferred to a 20 ml Teflon reactor and kept at 160 °C for 5 days under autogenous pressure, and cooled to room temperature at a rate of 10 °C/h. Red block crystals of compound **1** were obtained (76.8 mg, yield: 33.6% based on Cu). Anal. Calcd. for **1** (%): C, 26.26; H, 1.76; N, 6.13; Cu, 13.90; Mo, 3.50; W, 33.50%; Found: C, 26.11; H, 1.95; N, 6.28; Cu, 13.74; Mo, 3.35; W, 33.74. The preparation of **2** was similar to that of **1** except that $K_5[BW_{12}O_{40}]\cdot 15H_2O$ (420 g, 0.12 mmol) was used instead of $(NBu_4)_3[MoW_5O_{19}]$, and the pH value of the mixture was adjusted to 6.5. Brown block crystals of compound **2** were obtained (178.7 mg, yield: 58.8% based on Cu). Anal. Calcd. for **2** (%): C, 18.75; H, 1.30; N, 4.37; Cu, 9.92; W, 49.2%; Found: C, 18.52; H, 1.43; N, 4.48; Cu, 9.80; W, 49.01.

2.3. X-ray crystallography

The crystallographic data were collected at 293 K for **1** and 150 K for **2** on a Rigaku R-axis Rapid IP diffractometer using graphite monochromatic Mo$K\alpha$ radiation (λ=0.71073 Å) and IP technique. The structures were solved by the direct method and refined by the Full-matrix least squares on F^2 using the SHELXL-97 software [21]. The hydrogen atoms for water molecule were not located but were included in the structure factor calculations. Carbon and the nitrogen-bound hydrogen atoms were placed in geometrically calculated positions. The crystal data and structure refinements of compounds **1** and **2** are summarized in Table 1.

CCDC-671761 and CCDC-671760 contain the supplementary crystallographic data for this paper. These data can be obtained free of charge at www.ccdc.cam.ac.uk/conts/retrieving.html or from the Cambridge Crystallographic Data Centre, 12, Union Road, Cambridge CB2 1EZ, UK; Fax: +44-1223/336-033; E-mail: deposit@ccdc.cam.ac.uk.

3. Results and discussion

3.1. Synthesis

In this paper, two entangled compounds: $[(bpy)_6Cu^{I}_6Cl_3(Mo^{V}W_5O_{19})]$ (**1**) and $[(bpy)_7Cu^{I}_7Cl_2(BW_{12}O_{40})]\cdot H_2O$ (**2**), have been synthesized by using POMs as precursors under hydrothermal conditions. Compound **1** is an unprecedented eight-connected self-penetrating network, obtained by reaction of the Lindquist-type polyoxoanion $[Mo^{V}W_5O_{19}]^{3-}$ with the bpy ligand and $CuCl_2\cdot 2H_2O$. Under the similar experimental conditions, an interesting fivefold interpenetrating network is obtained by the use of the −5 valence Keggin-type $[BW_{12}O_{40}]^{5-}$. As well known, many entangled compounds have been synthesized by use of the polyoxoanions with the smaller volume, such as $[P_4Mo_6O_{25}(OH)_6]$ [18], Keggin-type polyoxoanion and its derivatives [16,17]. In the preparation, these polyoxoanions could offer smarter coordination sites and less steric hindrance than the Dawson polyoxoanion and other larger polyoxoanions. Additionally, we have obtained a fivefold interpenetrating network by the use of the Keggin heteroblue $[PW^{VI}_{10}W^{V}_2O_{40}]^{5-}$ with the −5 valence. Also, we have tried to synthesize the interpenetrating network by using $[PW_{12}O_{40}]^{3-}$ and $[SiW_{12}O_{40}]^{4-}$ as the start materials. However, no entangled compounds can be obtained after several months of attempts. It can be concluded that the volume and charge differences of these two polyoxoanions play important roles in constructing these two compounds. Further, the pH value also affects the synthesis of title compounds. A series of parallel synthetic experiments indicate that compound **1** can be obtained in the pH range of 4–5, while **2** could be isolated in the pH range of 6.5–7.5. Additionally, the presence of Cu^+ ions in these two compounds indicates that the starting Cu^{2+} ions are reduced by the NH_4Cl and bpy ligands, which has been observed in the previous reports [22–24].

Table 1
Crystal data and structure refinement for **1** and **2**.

	1	**2**
Empirical formula	$C_{60}H_{48}Cl_3N_{12}O_{19}Cu_6MoW_5$	$C_{70}H_{58}BCl_2Cu_7N_{14}O_{41}W_{12}$
Formula weight	2743.88	4483.99
T (K)	293(2)	150(2)
Crystal system	Triclinic	Triclinic
Space group	$P1$	$P1$
a (Å)	11.502(2)	12.341(3)
b (Å)	13.069(3)	13.119(3)
c (Å)	13.296(3)	15.367(3)
α (°)	90.55(3)	99.12(3)
β (°)	113.74(3)	90.53(3)
γ (°)	110.48(3)	104.49(3)
V (Å^3)	1687.4(6)	2375.4(8)
Z	1	1
D_c (Mg m^{-3})	2.700	3.135
Data/restraints/ parameters	7624/330/482	8048/495/610
R_{int}	0.0647	0.0955
$R_1(I>2\sigma(I))$[a]	0.0442	0.0796
wR_2 (all data)[a]	0.1174	0.1633
Goodness-of-fit on F^2	1.074	1.051

[a] $R_1=\sum||F_0|-|F_C||/\sum|F_0|$; $wR_2=\sum[w(F_0^2-F_C^2)^2]/\sum[w(F_0^2)^2]^{1/2}$.

3.2. Structure description

Crystal structure of **1**: Single crystal X-ray diffraction analyses reveal that compound **1** exhibits an eight-connected self-penetrating network constructed from metal–organic framework consisting of the cuprous chloride clusters $[Cu_6Cl_3]$ and bpy ligands, and the zigzag chains based on polyoxoanions [MoVW5O19]$^{3-}$ and bpy ligands. In the $[Cu_6Cl_3]$ cluster (see Fig. S1a), six Cu(I) ions can be divided into two groups according to their coordination modes. The first group Cu(1), Cu(1A), Cu(2) and Cu(2A) ions are all in the tetrahedral coordinated environment completed by two chlorine atoms (average bond length of Cu–Cl 2.24(2) Å) and two nitrogen atoms derived from two bpy

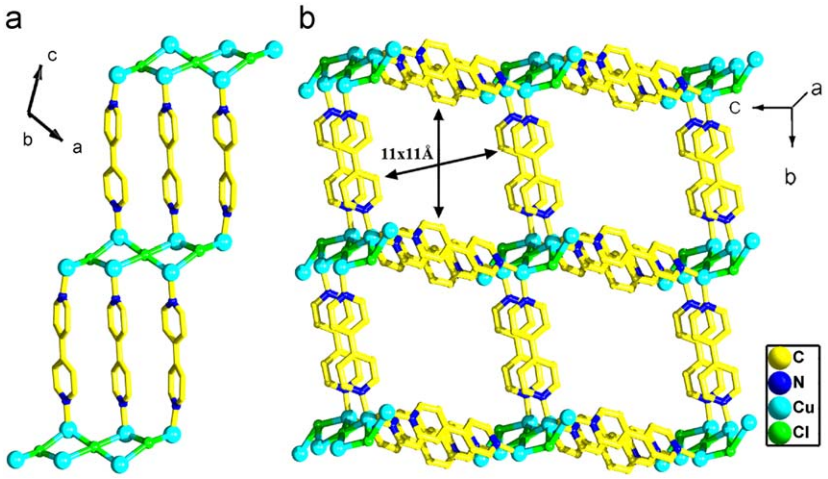

Fig. 1. Ball-and-stick representations of 2D layer (a) and the 3D network (b) of **1**.

molecules (average bond length of Cu–N 2.01(8) Å). In the four tetrahedra, the Cu(1) tetrahedron is edge-sharing with the Cu(2A) tetrahedron to form a dimer, which is corner-sharing with a same dimer composed of the Cu(1A) and Cu(2) to constitute a Cu_4 unit. The second group Cu(3) and Cu(3A) are all coordinated to one chlorine atom (Cu(3)–Cl(1) 2.687(3) Å), two pyridyl nitrogen donors and one oxygen atom from $[Mo^{V}W_5O_{19}]^{3-}$ (Cu(3)–O(3) 2.438(5) Å) to form a distorted tetrahedral geometry. Two distorted tetrahedra $CuClN_2O$ are located on both sides of the Cu_4 unit to form a nearly coplanar Cu_6 cluster with idealized C_i symmetry (see Fig. S1b). The neighboring $[Cu_6Cl_3]$ clusters are linked together by three nearly parallel bpy molecules to form 2D layers (see Fig. 1a), which are further pillared via two nearly parallel bpy molecules to construct the 3D network possessing of the quadrilateral channels with the sizes of 11.0×11.0 Å^3 (see Fig. 1b). The bpy molecules located on diagonals of the quadrangles join the 3D networks together through the Cu(3) ion to generate a novel metal–organic framework (see Fig. S2). As well known, no analogous metal–organic framework composed of the $[Cu_6Cl_3]$ clusters and bpy molecules has been reported in the literatures.

In one 3D network, each quadrilateral channel can accommodate one polyoxoanion $[Mo^{V}W_5O_{19}]^{3-}$, which is the mono-Mo-substituted Lindquist type POM (Fig. S3). The Mo and W atoms in the anion $[Mo^{V}W_5O_{19}]^{3-}$ are all in the octahedral coordinated environment and share one central μ_6-O atom. As shown in Fig. S3, each octahedron is edge-sharing with four adjacent ones. It is noteworthy that four metal centers on the Lindquist anion exhibit the site-occupancy disorder with 25% of Mo and 75% of W, respectively. In compound **1**, each polyoxoanion $[Mo^{V}W_5O_{19}]^{3-}$ acts as a bidentate ligand connecting by the two Cu^{+} ions with two bpy molecules to form a zigzag chain (see Fig. S3). These zigzag chains penetrated the 3D networks and bridged them into a self-penetrating framework (see Fig. 2a). Further, the $[Cu_6Cl_3]$ cluster can be abstracted as an eight-connected node which linked with eight nearest neighbors at distances of 13.069–20.415 Å (see Figs. 2b and c), resulting in a novel 3D uninodal framework of $4^{24}56^3$ topology (see Fig. 2d).

Notably, the structure of **1** is completely different from that of the familiar body-centered cubic lattice (bcu) [25]. In bcu, the zigzag chain in the interlayer region bridges across the diagonal of a single window in the (4,4) net. In **1**, it bridges the diagonal of two windows (Fig. 2e). As a result, the shortest catenated four-membered rings are observed at the intersection of the 2D layers. The resulting array is a single eight-connected self-penetrating network (Fig. 2d).

By far, only three eight-connected self-penetrating organic–inorgainc hybrids have been reported. We have reported two compounds: $[Zn_5(\mu_3\text{-}OH)_2(bdc)_4(phen)_2]$ (phen=1,10-phenanthroline) with $4^{24}56^3$ topology [26] and $[Cd_3(bdc)_3(L)_2(H_2O)_2]$ with $4^{20}6^8$ topology [27]. Recently, Xu and co-workers reported one compound $[Cu_4(bpp)_4V_4O_{12}]$ with $4^{24}6^4$ topology [28]. It is noteworthy that eight-connected nodes in the above three compounds are composed of multi-nuclear metal–oxygen clusters, while in **1** metal–halide clusters act as eight-connected nodes for the first time. Very recently, a pure inorganic eight-connected POM-based aggregate was reported [29]. Accordingly, compound **1** represents the first POM-based eight-connected self-penetrating organic–inorganic hybrids.

Crystal structure of **2**: Compound **2** exhibits an interesting fivefold interpenetrating network structure consisting of five equivalent 3D nets (Fig. 3). Each single net is built from coordination polymer layers based on Cu(I) ions, chlorine atoms, bpy molecules and Keggin-type polyoxoanion $[BW_{12}O_{40}]^{5-}$ (Fig. 4 and S4-8). The fivefold interpenetrating network is isostructural to that of a reduced POM $[PW^{VI}_{10}W^{V}_{2}O_{40}]$-containing compound $[(bpy)_7Cu^{I}_7Cl_2(PW^{VI}_{10}W^{V}_{2}O_{40})]$ (**3**) [17]. To our knowledge, these compounds represent the highest degree of interpenetration presently known for POM system.

3.3. IR, TG Analyses, XPS, XRD and Electrochemical Analyses

In the IR spectrum of **1**, the characteristic peaks at 988, 950, 816, 794, 726, 579, and 445 cm^{-1} are attributed to ν(M=O) and ν(M–O–M) (M=Mo or W) of $[Mo^{V}W_5O_{19}]^{3-}$ polyoxoanion [19] and the characteristic bands at 3551, 3093, 1614, 1603, 1532, 1484, 1408, 1323, 1219, and 1066 cm^{-1} can be regarded as features of the bpy molecule (Fig. S9a). In the IR spectrum of compound **2**, the characteristic peaks at 996, 952, 899, 826, 804, 647, 531, and 423 cm^{-1} are attributed to ν(B–Oa), ν(W–Od), ν(W–Oa), ν(W–Ob) and ν(W–Oc) of the $[BW_{12}O_{40}]^{5-}$ polyoxoanion and the characteristic bands at 3523, 3098, 1605, 1530, 1487, 1415, 1322, 1220, and 1069 cm^{-1} can be regarded as features of the bpy molecule (Fig. S9b).

TG curve of **1** (Fig. S10a) shows that chemical decomposition starts at 360 °C and ends at 606 °C with the weight loss of 34.50%, equivalent to the loss of all the organic ligands (calcd 34.15%). TG curve of **2** (Fig. S10b) shows two weight loss steps from 140–768 °C. The first weight loss is 0.64% in the temperature range 140–230 °C, corresponding to the release of one lattice water molecule. The second weight loss of 23.82% in the

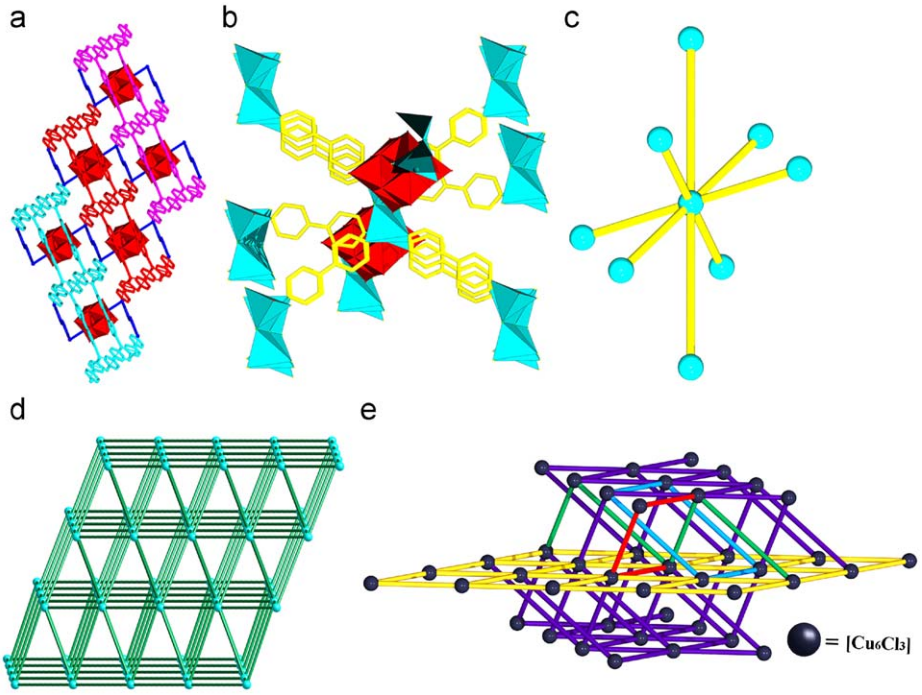

Fig. 2. The detailed structures in **1**. (a) Ball-and-stick representation of 3D self-penetrating in **1** color modes: zigzag chain, blue; (b) perspective and (c) simplified views of the eight-connecting $[Cu_6Cl_3]$ cluster, (d) topological representation of **1** showing the $4^{24}56^3$ topology. The $[Cu_6Cl_3]$ clusters are represented by turquoise balls and (e) schematic representation illustrating the linking modes between the 4^4 nets in the eight-connected nets of **1**. The self-penetrating shortest circuits are highlighted. (For interpretation of the references to the color in this figure legend, the reader is referred to the web version of this article.)

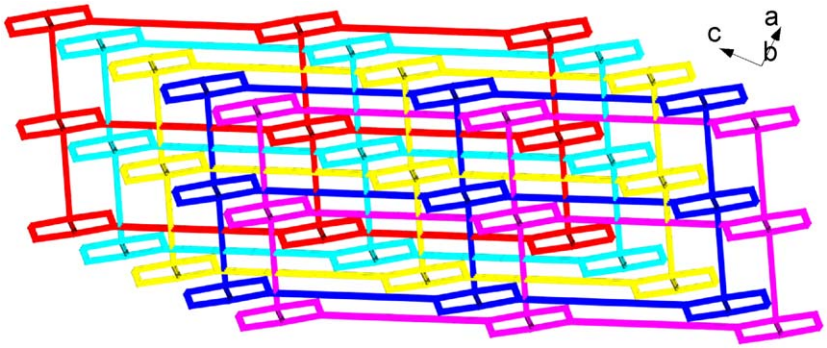

Fig. 3. Polyhedral and ball-and-stick representation of 3D network of **2** along different directions.

temperature range 340–768 °C, attributed to the loss of all the organic ligands. The whole weight loss (24.46%) is in good agreement with the calculated value (24.78%).

X-ray photoelectron spectra (XPS) were performed to identify the oxidation states of Cu atoms in compounds **1** and **2**. XPS for **1** (see Fig. 5a) exhibits two peaks of ca. 931.9, and ca. 951.9 eV in the energy region of $Cu2p_{3/2}$ and $Cu2p_{1/2}$, consistent with the Cu^+oxidation state [24]. The XPS for **2** (see Fig. 5b) also show the similar peaks in the energy region of $Cu2p_{3/2}$ and $Cu2p_{1/2}$, confirming that all the Cu centers in two compounds possess the +1 oxidation state. These results are in agreement with the BVS calculations and the charge balance consideration (Table S1) [30]. Also, the purity of two compounds has been confirmed by the X-ray powder diffraction (XRD). The XRD patterns of the as-synthesized are almost identical to the calculated pattern from single-crystal diffraction data (Figs. S11 and S12). Only diffraction peak intensities and widths show some variations, revealing that that the single crystal is representative of the bulk sample.

To study the redox property of **2**, **2**-bulk-modified carbon paste electrode (**2**-CPE) was fabricated as the working electrode owing to its insolubility in water and most organic solvents. Cyclic voltammetry on **2**-CPE was carried out in a pH=2.5 (1 M LiCl+0.5 M H_2SO_4) solution in the potential range from −1.4 to +0.5 V. The cyclic voltammetric behaviors of **2** exhibits four reduction peaks in the potential range of +0.5 ~ −1.4 V and the mean peak potentials are −0.169, −0.793, −1.045 and −1.264 V (vs. Ag/AgCl), respectively (Fig. 6). The first one reduction peak located at −0.169 V and its oxidation counterpart are attributed to the redox processes of the Cu^+ centers. The last three reduction peaks are attributed to the redox processes of the W^{6+}centers [31]. When the scan rates were lower than 300 mV s^{-1}, the peak currents of W reduction waves were proportional to the scan rates, indicating that the redox process on the **2**-CPE is surface-controlled [32].

4. Conclusions

In summary, we have successfully synthesized two entangled compounds (**1** and **2**) under hydrothermal conditions. Compound

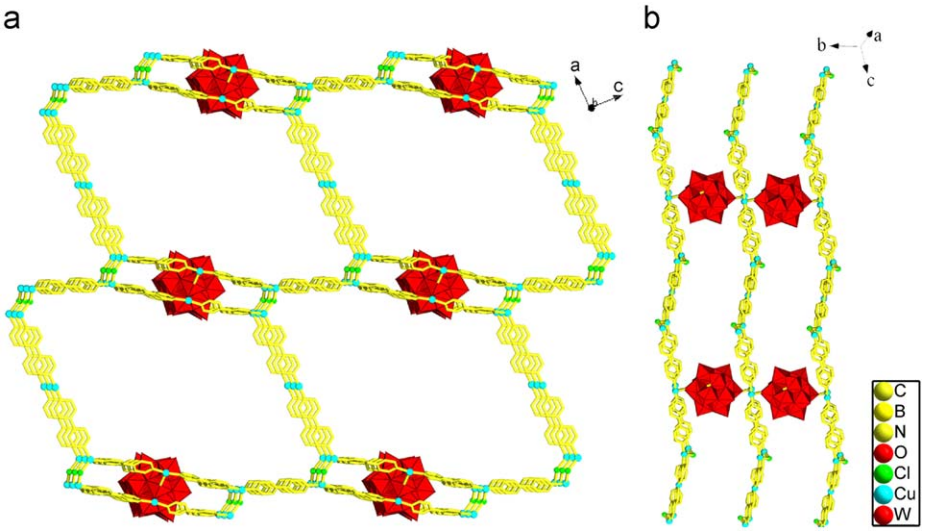

Fig. 4. Topological view of the fivefold parallel interpenetration for **2**.

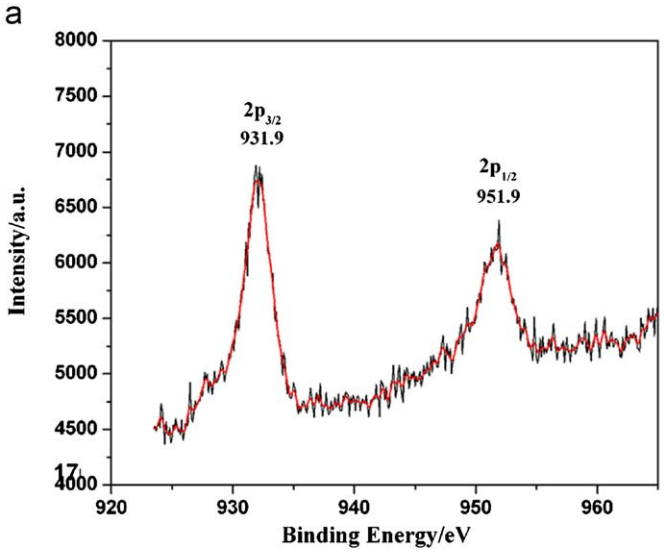

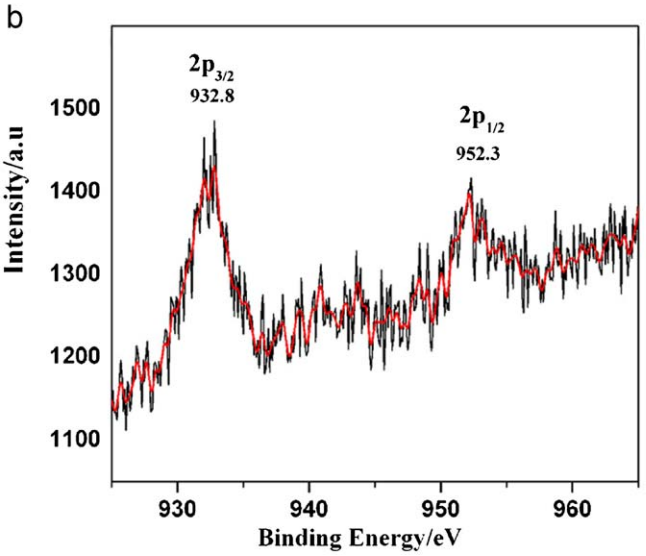

Fig. 5. The XPS spectra for **1** (a) and **2** (b).

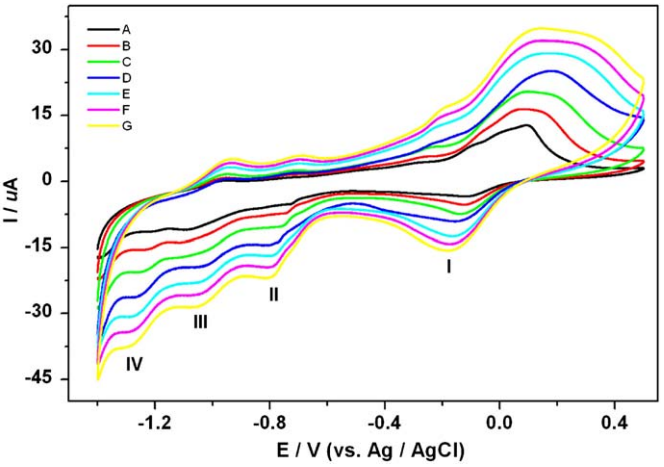

Fig. 6. Cyclic voltammogram of **2** in a pH=2.5 (1 M LiCl+0.5 M H_2SO_4) solution at the scan rates (from inner to outer: 20, 50, 100, 150, 200, 250 and 300 mV s^{-1}).

1 represents the first POM-based eight-connected self-penetrating organic–inorganic hybrid network. Compound **2** has an interesting fivefold interpenetrating network structure consisting of five equivalent 3D interwoven nets. The variety of such entangled compounds might be adjusted by choice of different POMs, transition metal ions and organic ligands. Further study in this field is underway.

Supporting information available

The IR spectrums, the TG curves, additional figures tables of **1** and **2** are available.

Acknowledgments

The Postdoctoral station Foundation of Ministry of Education (No. 20060200002) and the Program for Changjiang Scholars and Innovative Research Team in University.

Appendix A. Supplementary data

Supplementary data associated with this article can be found in the online version at 10.1016/j.jssc.2009.10.016.

References

[1] J.P. Sauvage, C. Dietrich-Buchecker, Molecular Catenanes, Rotaxanes and Knots, A Journey Through the World of Molecular Topology, Wiley-VCH, Weinheim, 1999.
[2] S.R. Batten, R. Robson, Angew. Chem. Int. Ed. 37 (1998) 1460–1494.
[3] L. Carlucci, G. Ciani, D.M. Proserpio, Coord. Chem. Rev. 246 (2003) 247–289.
[4] S.A. Bourne, J. Lu, B. Moulton, M.J. Zaworotko, Chem. Commun. (2001) 861–862.
[5] X.H. Bu, M.L. Tong, H.C. Chang, S. Kitagawa, S.R. Batten, Angew. Chem. Int. Ed. 43 (2004) 192–195.
[6] P. Jensen, D.J. Price, S.R. Batten, B. Moubaraki, K.S. Murray, Chem. Eur. J. 17 (2000) 3186–3195.
[7] L. Carlucci, G. Ciani, D.M. Proserpio, F. Porta, Angew. Chem. Int. Ed. 42 (2003) 317–322.
[8] D.L. Long, E. Burkholder, L. Cronin, Chem. Soc. Rev. 36 (2007) 105–121.
[9] M.T. Pope, Heteropoly and Isopoly Oxometalates, Springer, Berlin, 1983.
[10] C. Ritchie, E. Burkholder, P. Kögerler, L. Cronin, Dalton Trans. (2006) 1712–1714.
[11] D. Hagrman, C. Zubieta, R.C. Haushalter, J. Zubieta, Angew. Chem. Int. Ed. 36 (1997) 873–876.
[12] A. Dolbecq, P. Mialane, L. Lisnard, J. Marrot, F. Sécheresse, Chem. Eur. J. 9 (2003) 2914–2920.
[13] J. Tao, X.M. Zhang, M.L. Tong, X.M. Chen, J. Chem. Soc. Dalton Trans. (2001) 770–771.
[14] X.L. Wang, C. Qin, E.B. Wang, Angew. Chem. Int. Ed. 43 (2004) 5036–5040.
[15] X.L. Wang, C. Qin, E.B. Wang, Angew. Chem. Int. Ed. 44 (2005) 5824–5827.
[16] X.L. Wang, C. Qin, E.B. Wang, Z.M. Su, Chem. Commun. (2007) 4245–4247.
[17] L.L. Fan, D.R. Xiao, E.B. Wang, Y.G. Li, Z.M. Su, X.L. Wang, Cryst. Growth Des. 7 (2007) 592–594.
[18] J. Liu, E.B. Wang, X.L. Wang, D.R. Xiao, L.L. Fan, J. Mol. Struct. 876 (2008) 206–210.
[19] C. Sanchez, J. Livage, J.P. Launay, M. Fournier, Y. Jeannin, J. Am. Chem. Soc. 104 (1982) 3194–3202.
[20] C.R. Deitcheff, M. Fournier, R. Franck, R. Thouvenot, Inorg. Chem. 22 (1983) 207–216.
[21] G.M. Sheldrick, SHELXL97, Program for Crystal Structure Refinement, University of Göttingen, Göttingen, Germany, 1997;
G.M. Sheldrick, SHELXS97, Program for Crystal Structure Solution, University of Göttingen, Göttingen, Germany, 1997.
[22] P. Pyykkö, Chem. Rev. 97 (1997) 597–636.
[23] A.N. Khlobystov, A.J. Blake, N.R. Champness, D.A. Lemenovskii, A.G. Majouga, N.V. Zyk, M. Schröder, Coord. Chem. Rev. 222 (2001) 155–192.
[24] C.M. Che, Z. Mao, V.M. Miskowski, M.C. Tse, C.K. Chan, K.K. Cheung, D.L. Phillips, K.H. Leung, Angew. Chem. Int. Ed. 39 (2000) 4084–4088.
[25] O.D. Friedrichs, M. O'Keeffe, O.M. Yaghi, Acta Crystallogr. Sect. A 59 (2003) 22–27.
[26] X.L. Wang, C. Qin, E.B. Wang, Z.M. Su, Chem. Eur. J. 12 (2006) 2680–2691.
[27] X.L. Wang, C. Qin, E.B. Wang, Z.M. Su, X. Lin, S.R. Batten, Chem. Commun. (2005) 4789–4791.
[28] X.S. Qu, L. Xu, G.G. Gao, F.Y. Li, Y.Y. Yang, Inorg. Chem. 46 (2007) 4775–4777.
[29] H. Tan, W. Chen, Y. Li, D. Liu, L. Chen, E. Wang, J. Solid State Chem. 182 (2009) 465–470.
[30] The valence sum calculations are performed on a program of bond valence calculator, version 2.00 February 1993, written by C. Hormillosa, with assistance from Healy, S. distributed by I.D. Brown.
[31] L. Cheng, X.M. Zhang, X.D. Xi, B.F. Liu, S.J. Dong, J. Electroanal. Chem. 407 (1996) 97.
[32] B. Keita, P. Mialane, F. Sécheresse, P. Oliveira, L. Nadjo, Electrochem. Commun. 9 (2007) 164.